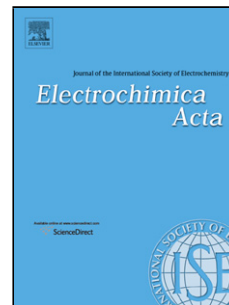


Accepted Manuscript

Title: Electrocatalytic dechlorination of chloropicolinic acid mixtures by using palladium-modified metal cathodes in aqueous solutions

Author: Hongxing Ma Yinghua Xu Xufen Ding Qi Liu
Chun-An Ma



PII: S0013-4686(16)31318-4
DOI: <http://dx.doi.org/doi:10.1016/j.electacta.2016.06.001>
Reference: EA 27440

To appear in: *Electrochimica Acta*

Received date: 24-2-2016
Revised date: 30-5-2016
Accepted date: 1-6-2016

Please cite this article as: Hongxing Ma, Yinghua Xu, Xufen Ding, Qi Liu, Chun-An Ma, Electrocatalytic dechlorination of chloropicolinic acid mixtures by using palladium-modified metal cathodes in aqueous solutions, *Electrochimica Acta* <http://dx.doi.org/10.1016/j.electacta.2016.06.001>

This is a PDF file of an unedited manuscript that has been accepted for publication. As a service to our customers we are providing this early version of the manuscript. The manuscript will undergo copyediting, typesetting, and review of the resulting proof before it is published in its final form. Please note that during the production process errors may be discovered which could affect the content, and all legal disclaimers that apply to the journal pertain.

Electrocatalytic dechlorination of chloropicolinic acid mixtures by using palladium-modified metal cathodes in aqueous solutions

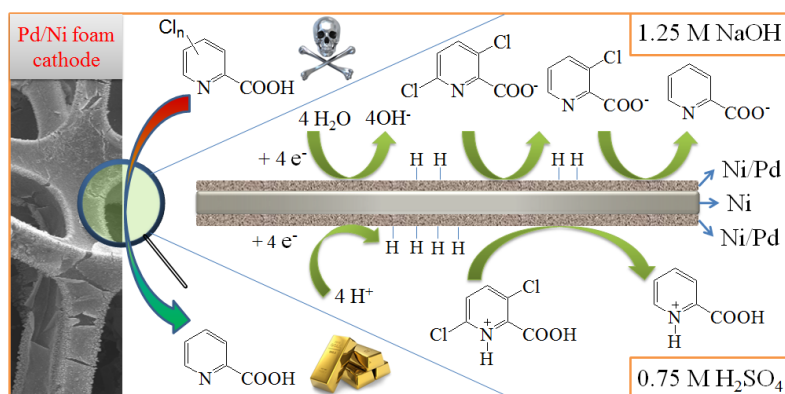
Hongxing Ma^a, Yinghua Xu^{a*}, Xufen Ding^a, Qi Liu^b, Chun-An Ma^{a*}

^aState Key Laboratory Breeding Base of Green Chemistry-Synthesis Technology, College of Chemical Engineering, Zhejiang University of Technology, Hangzhou City, Zhejiang 310032, China

^bCollege of Life and Environmental Science, Hangzhou Normal University, Hangzhou City, Zhejiang 310036, China

*Corresponding author. Tel & Fax: +86-0571-88320830. E-mail: xuyh@zjut.edu.cn (Y. Xu), science@zjut.edu.cn (C. Ma)

Graphical abstract



ABSTRACT

In China, chloropicolinic acid (CIPA) mixtures comprising 3,5,6-trichloropicolinic acid, 3,6-dichloropicolinic acid (3,6-D), 3-CIPA, and 6-CIPA are discharged as organic wastes at a rate of approximately 300 tons per year. In this work, we developed an aqueous phase electrocatalytic hydrogenation (ECH) system based on Pd catalyst to dechlorinate the CIPA mixtures into picolinic acid (PA) at room temperature. Firstly, we evaluated the influence of cathode support and Pd loading on the catalytic performance of cathodes, as well as the effects of operating parameters on the intermediate product selectivity and dechlorination efficiency of the ECH process with 3,6-D as the target compound. Secondly, we analyzed the ECH dechlorination mechanism of 3,6-D with regard to the surface condition of cathode and catholyte pH, and the rate-limiting step of the dechlorination process was also discussed. Finally, we assessed the practicability of the ECH system to dechlorinate the CIPA mixtures into PA by using a plate-and-frame cell. Results demonstrated that Pd/Ni foam cathodes with Pd loading of 2.25–3.6 mg cm⁻² exhibited the optimum ECH dechlorination performance, and the basic aqueous solution and high 3,6-D concentration favored the ECH process. The CIPA mixtures with 47 g L⁻¹ concentration (the total concentration of CIPAs was approximately 250 mM) can be selectively dechlorinated into PA with 99% yield, 76.3% current efficiency, and 2.47

$\text{kW}\cdot\text{h}\cdot\text{kg}^{-1}$ PA specific electric energy consumption at a current density of 208 A m^{-2} in a 1.25 M NaOH aqueous solution.

Keywords: 3,6-Dichloropicolinic acid; High concentration; Electrocatalytic dechlorination; Pd/Ni foam; Dechlorination mechanism

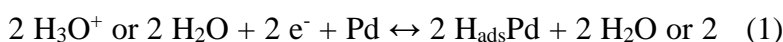
1. Introduction

China is one of the largest producers of 3,6-dichloropicolinic acid (3,6-D), a selective herbicide used to control broadleaf weeds, particularly thistles and clovers. Recently, the total production of 3,6-D in China has reached up to 3000 tons per year [1-3], and past trends indicate further increase in global production and application of this herbicide. Since 2010, the electrochemical reduction of 3,4,5,6-tetrachloropicolinic acid has become the main source of 3,6-D in China because of its high yield and relatively low environmental contamination [4]. However, the process have to discharge chloropicolinic acid (CIPA) mixtures containing 3,5,6-trichloropicolinic acid (3,5,6-T), 3,6-D, 3-CIPA, and 6-CIPA as organic wastes. In a typical electrochemical synthesis process, these compounds are present in ratios of 1 wt%, 82 wt%, 7 wt%, and 6 wt%, resulting in approximately 0.1 ton of CIPA mixtures per ton of pure 3,6-D product.

Several oxidation techniques such as photocatalysis [5], electro-Fenton [6], electron beam treatment [7], and UV/H₂O₂ or ozone treatment [8] have been suggested for the disposal of 3,6-D. Therefore, these techniques may also be applicable to the degradation of CIPA mixtures. In principle, however, reductive dechlorination techniques are more suitable than oxidation techniques in treating CIPA mixtures because of the possibility of transforming these mixtures into highly valuable products, such as picolinic acid (PA), the price of which amounts to approximately 30,000 USD per ton. Numerous reduction techniques have been

reported for the dechlorination of chlorinated organic compounds (COCs); these strategies include microbial dechlorination [9], zero-valent metal [10] or modified zero-valent metal reduction [11], and catalytic hydrodechlorination [12]. Among these, catalytic hydrodechlorination with Pd/Al₂O₃ catalyst has been proven to be an effective method to transform 3,6-D into PA (77% yield) [12].

Compared with the above methods, electrocatalytic hydrogenation (ECH) presents a significant potential to transform ClPA mixtures into PA in an industrial scale because ECH provides mild reaction conditions without the secondary pollution effects associated with excess reagents. In the past 10 years, ECH dechlorination with Pd as electrocatalyst has been proven to be one of the most attractive methods for the disposal of hazardous COCs [13-19]. In accordance with the literature [15-17], the ECH dechlorination process is described in Eqs. (1)–(4) (where M refers to Pd or supports):



In virtue of the specific interactions between Pd and hydrogen, a strongly reducing adsorbed hydrogen (H_{ads}) can be electro-generated in situ at very positive potentials and is quite active toward the hydrodechlorination of C-Cl. Almost all types of C-Cl, including C_{sp3}-Cl (aliphatic chlorides [18]) and C_{sp2}-Cl (aryl [17] or alkenyl chlorides [19]), can be hydrogenated with H_{ads}. These two facts make it possible to dechlorinate various COCs with very low electric energy consumption. In addition, the Pd electrocatalyst support exerts a major effect on the ECH dechlorination performance of Pd-modified cathodes because it influences the electronic structure of the catalyst (Pd) [20] and may change the adsorption behavior of the reactant (R-Cl) [21]. Therefore, numerous materials have been investigated as potential electrocatalyst supports. These items mainly include different metal materials such as Ti mesh [22], Ti/TiO₂ nanotubes [19], Fe gauze [23], Ag mesh [16,17], Cu foam [24], and Ni foam

[13,14,24-27]; various carbon-based materials such as glassy carbon (GC) [15], reticulated vitreous carbon (RVC) [28], MoO_x-modified GC [29], activated carbon fibre/cloth [30,23,31], granular graphite [32], carbon nanotubes [33] and graphene [34-35]; and other composite materials such as polypyrrole [36], polypyrrole/Ni foam [37-39], and surfactant/polypyrrole/meshed Ti [40].

In this paper, we primarily report the ECH dechlorination of 3,6-D (as the representative of CIPA mixtures) in aqueous solutions at room temperature by using Pd/Ni foam cathodes. High concentrations of 3,6-D (25–300 mM) were used in our work for the practicability of ECH dechlorination. Our study mainly aims to develop a highly efficient ECH dechlorination system (by optimizing the ECH dechlorination conditions, such as cathode materials, pH of catholyte, initial concentration of 3,6-D, and applied current density) and evaluate the practicability of this system to convert CIPA mixtures into PA. Furthermore, this research aims to determine the reaction mechanism of 3,6-D and the rate-limiting step in the ECH dechlorination system. To our knowledge, this study is the first to employ an ECH technique with Pd-modified cathode in the dechlorination of CIPA. In addition, studies on Pd-modified cathodes have focused predominantly on the in-situ treatment of ubiquitous COCs existing in trace amounts; however, the use of the ECH dechlorination technique to dispose high concentrations of COCs (>70 mM) has not been reported to date [31].

2. Materials and methods

2.1. Chemicals

Ni foams (1.0 mm thickness), Cu foams (1.0 mm thickness), and Ag mesh (open area 37%) were obtained from Cells Electrochemistry Experiment Equipment Co., Ltd., China (www.hzcell.com). 3,5,6-T, 3,6-D, 3-CIPA, 6-CIPA, and PA with purity of 98%–99% and CIPA mixtures comprising 3,5,6-T (1.3 wt%), 3,6-D (81.6 wt%), 3-CIPA (6.5 wt%), 6-CIPA (6.4 wt%), and PA (0.4 wt%) were obtained from Zhejiang Avilive Chemical Co., Ltd., China (www.avilive.com) and used as received. PdCl₂ (99.5 wt%), NaOH, HCl, H₂SO₄, KH₂PO₄, H₃PO₄, acetone, and ethanol, all

with 97 wt%–99 wt% purity, were obtained from Aladdin Reagent Co., China and used as received. Acetonitrile and methanol (HPLC grade) used for HPLC analysis were purchased from National Medicines Co., Ltd., China. H₂O with resistivity of 18.2 M Ω ·cm was obtained from a Millipore Milli-Q system for the preparation of all solutions.

2.2. Electrode modification

Pd-modified nickel (Pd/Ni) foam, silver (Pd/Ag) mesh, and copper (Pd/Cu) foam electrodes were prepared by electroless deposition, which was conducted spontaneously via a galvanic replacement reaction until the yellow PdCl₂ solution turned colorless with the vial capped and the solution stirred. Prior to Pd modification, three electrode supports were degreased and cleansed in acetone for 20 min under ultrasonic vibration and then etched in a diluted H₂SO₄ (80 g L⁻¹) solution for 5 min to remove surface native oxides. After thorough rinsing with deionized water, the supports were immersed into a vial with 50 mL aqueous solution of 0.1 M HCl containing different concentrations of PdCl₂ at 25 °C. A number of electrodes were deposited under exactly the same conditions to ensure reproducibility. After Pd modification, the electrodes were kept in ethanol for later use without drying.

2.3. Apparatus

The surface morphology and composition of the abovementioned electrodes were determined by SEM (Scanning Electron Microscope, Hitachi S-4700 II) equipped with EDS (Energy Dispersive Spectrometer, Thermo NOANVANTAGE ESI) and XRD (X-Ray Diffraction, Thermo ARLSCINTAG X'TRA, 45 kV and 40 mA, Cu K α). XPS (KRATOS AXIS ULTRA DLD) with a monochromatized aluminium X-ray source was used to confirm the Pd element surface concentration of Pd/Ni foam. The binding energies were calculated with C1s peak (284.8 eV) as internal standard.

Cycle voltammetry (CV) and electrolysis experiments were conducted with a PAR 283 potentiostat and a DC-regulated power supply (HZC-061), respectively. A three-electrode cell composed of a Ag/AgCl reference electrode, a Pt (2 cm × 2 cm) counter electrode, and a Pd/Ni disk working electrode (3 mm diameter) was used for the CV experiments. The potentials of the CV experiments were reported relative to the Ag/AgCl/saturated KCl aqueous solution reference.

A conventional two-compartment glass H-cell separated by a Nafion-117 membrane was used in the electrolysis experiments to obtain the optimized ECH dechlorination conditions. The cathode and anode were manufactured from a material consisting of Ni foam, Ag mesh, Cu foam, Pd/Ni foam, Pd/Ag mesh or Pd/Cu foam (Projected area: 2 cm × 6 cm), and graphite sheet (2 cm × 6 cm). The volume of the catholyte and anolyte was 50 mL each, and the catholyte was stirred during electrolysis.

Density functional theory (DFT) was used to calculate C-Cl bond length of the 3,6-D molecular and to simulate its optimized molecular structure with the hybrid exchange functional of B3LYP [41]. For C, N, O, Cl and H, and the basis sets [42] were 6-311+ G (*d*, *p*). Gaussian 03 software package [43] was used to perform all the calculations and simulations.

A plate-and-frame cell with a Nafion-117 membrane was selected to assess the practicability of the ECH dechlorination system and convert the CIPA mixtures into PA. A piece of Pd/Ni foam (Projected area: 7 cm × 13 cm) in a 1.25 M NaOH aqueous solution containing 47 g L⁻¹ CIPA mixtures (total concentration of CIPAs: approximately 250 mM) was used as the cathode, and a stainless steel mesh (7 cm × 13 cm) in a 1.25 M NaOH aqueous solution was used as the anode. The schematic construction of the electrolysis device using the plate-and-frame cell is shown in Fig. 1. The volume of the catholyte and anolyte was 700 mL each.

All CV and electrolysis experiments were performed at 25 °C and a 1.25 M NaOH or 0.75 M H₂SO₄ aqueous solution was used as anolyte in all electrolysis experiments.

2.4. Analytical methods

A Waters HPLC system was used to analyze the dechlorinated products and the remaining reactants at room temperature. The system was assembled with a symmetry column (250 mm length \times 4.6 mm i.d., 5 μ m particle size), an injection valve fitted with a 20 μ L sample loop, and a Waters 2996 Photodiode Array Detector (λ 275 nm). Isocratic elution was used with a mobile phase of acetonitrile/methanol/H₂O (1:3:6 v/v) containing 30 mM H₃PO₄ at a flow rate of 1 mL \cdot min⁻¹. Calibration curves of standards were used to determine the concentrations of the product and the remaining reactants. The precision of the mass balance used in the measurement was ca. 97%–103% of the nominal value.

PA yield was calculated as the molar ratio of PA produced to the initial amount of 3,6-D. The conversion of 3,6-D was determined as the ratio of the amount of 3,6-D eliminated to the initial amount prepared. Current efficiency (CE, %) in the electrolysis of 3,6-D was calculated using the following equation:

$$CE = \frac{(n_1 \Delta C_{PA} + n_2 (\Delta C_{3-CIPA} + \Delta C_{6-CIPA})) FV}{I \times \Delta t}$$

where n_1 and n_2 are the electron transfer numbers per molecule of PA ($n_1 = 4$) and CIPA ($n_2 = 2$), respectively; ΔC_{PA} , ΔC_{3-CIPA} , and ΔC_{6-CIPA} are the concentration differentials (M) of PA, 3-CIPA, and 6-CIPA during Δt , respectively; F is the Faraday constant (96500 C \cdot mol⁻¹); V is the volume of the total catholyte (0.05 L); and I is the applied current.

A similar calculation method was used to obtain the yield of PA and the CE of the electrolysis of the CIPA mixtures. The specific electric energy consumption (SEEC, kW \cdot h \cdot kg⁻¹ PA) of the electrolysis process was calculated using the following equation:

$$SEEC = \frac{I \times \Delta t \times U}{\Delta C_{PA} \times V \times M}$$

where I is 1.89 A, Δt is 12 h, U is the average cell voltage (2.3 V), V is 0.7 L, and M is the relative molecular mass of PA.

3. Results and discussion

3.1. Effect of cathode material

3.1.1. Effect of cathode supports

We initially evaluated the effect of cathode supports on the dechlorination of 3,6-D through a series of electrolysis experiments. As shown in Table 1, higher CE and PA yield were obtained from the Pd/Ni foam cathode than those from the Pd/Ag mesh and Pd/Cu foam cathodes. A very small amount of 3,6-D was mainly dechlorinated into 6-ClPA when the Ni foam, Ag mesh, and Cu foam were used as cathodes. These results suggest that Pd is a powerful electrocatalyst for the dechlorination of 3,6-D, and the Pd/Ni foam is the most feasible cathode material for the dechlorination of 3,6-D among the three Pd-modified metal cathodes.

In addition, Cl at C6 of 3,6-D exhibited higher reductive activity than Cl at C3 on three Pd-modified metal cathodes, but an opposite activity order was exhibited on three metal cathodes. Pyridinic nitrogen is a stronger electron-withdrawing group than COO⁻; thus, Cl at C6 of 3,6-D would be more active than Cl at C3 of the isolated 3,6-D molecule. Therefore, the selectivity of the dechlorination reaction on the three metal cathodes was opposite to the directing effect of pyridinic nitrogen. This phenomenon would be interesting from the mechanistic viewpoint; however, this occurrence is not possible to analyze on the basis of the currently available data.

3.1.2. Effect of Pd loading

Considering that the Pd/Ni foam was the most feasible cathode material among the three Pd-modified metal cathodes, the effect of Pd loading on the dechlorination performance of the prepared Pd/Ni foam was further evaluated. As shown in Fig. 2, the conversion of 3,6-D reached 83% with the use of Pd/Ni foam cathode, which has very low Pd loading (0.45 mg cm^{-2}); whereas the optimal CE was achieved when the Pd/Ni foam cathodes with high Pd loading ($2.25\text{--}3.6 \text{ mg cm}^{-2}$) was used. These results indicate that the dechlorination activity of the Pd/Ni foam cathodes strongly depend on Pd loading, and a loading of 2.25 mg cm^{-2} favors the performance of the cathode to

save Pd use.

3.1.3. Dechlorination stability of the Pd/Ni foam optimized

The dechlorination stability of the optimized Pd/Ni foam was evaluated by six recycled electrolysis experiments. As shown in Fig. 3, only slight reductions were observed in the yield of PA and CE over the six cycles of electrolysis experiments. This result implies that the dechlorination activity of the optimized Pd/Ni foam was almost stable in the 36 hours of electrolysis experiments.

3.2. Effect of operating parameters

3.2.1. Effect of catholyte pH

The catholyte pH exhibited a surprising “V” effect on the dechlorination of 3,6-D (Table 2). Moderate dechlorination efficiencies were obtained in neutral and weak acidic aqueous solutions (Entries 4 and 5), whereas very high dechlorination efficiencies were achieved in 1.25 M NaOH and 0.75 M H₂SO₄ (Entries 1 and 7).

To reveal this “V” effect, the dynamic curves of reactant and product concentrations, as well as that of CE, during the dechlorination were separately determined in 1.25 M NaOH or 0.75 M H₂SO₄ (Fig. 4). Low concentration (96 mM) of 3,6-D was used to ensure its complete dissolution in the acidic solution before the dechlorination experiment started. Over 100% CE was achieved in 0.75 M H₂SO₄ (Fig. 4B') in the early stage of the dechlorination experiment (≤ 2 h). According to Faraday's law, the highest CE of an electrolysis experiment is 100%. Therefore, we assumed that a Pd-modified zero-valent Ni dechlorination process occurred in 0.75 M H₂SO₄, in which Ni was the reducing agent and Pd was the catalyst. To confirm this theory, we performed separate experiments using Ni foam or Pd/Ni foam as the potential reducing agent and/or catalyst under identical conditions. A considerable reduction of 3,6-D to PA with a conversion of 9.7% and a yield of 9.3% was observed when the Pd/Ni foam was used, whereas no obvious reduction of 3,6-D was observed where the Ni foam was used after six hours of reaction. The abovementioned results strongly suggest that the Pd-modified zero-valent Ni dechlorination process coexisted with the electrochemical dechlorination of 3,6-D in 0.75 M H₂SO₄, which is one of

the reasons for the “V” effect of the catholyte pH.

In addition, the product selectivity was completely different at the two pH levels during the electrolysis process (Fig. 4A and 4B), although very similar dechlorination efficiencies (over 90% 3,6-D had been transformed into PA) were obtained at the two pH levels after six hours of the reaction. Obviously, two Cl atoms in the 3,6-D molecule were eliminated stepwise in 1.25 M NaOH with 3-CIPA as main intermediate product, whereas the atoms were removed together in one step in 0.75 M H₂SO₄ (i.e., two Cl atoms of 3,6-D were dechlorinated at the same stage before the desorption of the monochlorinated PA into the bulk catholyte). Explanation will be proposed for the differences in the product selectivity in Section 3.3.3.

Considering the solubility of 3,6-D and the dechlorination efficiency, we chose 1.25 M NaOH aqueous solution as the catholyte in the succeeding experiments.

3.2.2. Effect of 3,6-D initial concentration

Table 3 shows the effect of the initial concentration of 3,6-D on the dechlorination process. Increasing the initial concentration of 3,6-D from 25 mM to 200 mM resulted in an increase in CE from 17.6% to 95.3%; the CE was kept constantly high at approximately 96% as the concentration of 3,6-D increased from 200 mM to 300 mM. These results suggest that high initial concentrations (200–300 mM) are favorable for the dechlorination of 3,6-D, which is an important conclusion because the dechlorination of high concentration COCs (> 70mM) on Pd-modified cathodes has not been reported so far. High concentration of COCs may retard the dechlorination reaction of the Pd-modified electrode [31], which is probably one of the reasons why studies using Pd-modified electrodes focus predominantly on the dechlorination of low concentration COCs.

Moreover, nearly 100% PA yield was achieved at the two low initial concentrations of the reactant (25 and 50 mM), although the applied charge was greater than the theoretical charge. This result suggests that the dechlorination system developed (Pd/Ni foam with a loading of 2.25 mg cm⁻² as the cathode and 1.25 M NaOH aqueous solution as the catholyte) here is more selective than the catalytic

hydrodechlorination system using the catalyst of Pd/Al₂O₃ [12]; the latter not only dechlorinated 3,6-D to PA but also hydrogenated PA to pipercolinic acid. Similar results were reported for the catalytic hydrodechlorination of 4-chlorophenol; phenol was the sole hydrodechlorination product from a Pd/Ni foam catalyst [44], whereas the produced phenol was further hydrogenated to cyclohexanone and cyclohexanol over a Pd/Al₂O₃ catalyst [45]. Additionally, Calvo et al. [46] found that phenol was the only product detected in the catalytic hydrodechlorination of 4-chlorophenol on unsupported Pd nanoparticles. They considered that Al₂O₃ affected the selectivity of hydrodechlorination reactions because of its interaction with Pd, provoking changes in the electronic density of Pd that would influence the strength of adsorption on the Pd active sites.

3.2.3. Effect of applied current density

In an attempt to study the effect of current density on dechlorination efficiency, a series of electrolysis experiments was carried out. As shown in Fig. 5, the highest dechlorination efficiency was obtained at the current density of 208 A m⁻² (geometric area), especially during the later periods of electrolysis. The increase of current density from 83 A m⁻² to 208 A m⁻² resulted in the slight decrease of CE and the substantial increase of PA yield, whereas the increase of current density from 208 A m⁻² to 250 A m⁻² led to the decrease of both CE and PA yield at the end of the electrolysis experiments.

3.3. ECH dechlorination mechanism

3.3.1. CV evidence

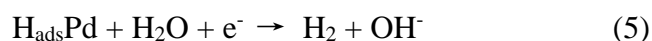
Fig. 6 shows the CV curves of Pd/Ni disk electrode in 1.25 M NaOH aqueous solution in the absence or presence of 3,6-D. In the absence of 3,6-D (Fig. 6A), the reductive peak (C1) associated with the electro-adsorption of hydrogen (Eq. 1, Section 1) and the reductive current response (C2) attributed to the absorption and evolution of hydrogen were detected in the negative potential going scan; in addition, a oxidative peak (A3) originated from the oxidation of particularly favourable sites on

the palladium surface, two oxidative peaks of adsorbed hydrogen (A2 and A2') and an oxidative peak of absorbed hydrogen (A1) were observed in the positive potential going scan [47]. In the presence of 3,6-D (Fig. 6B), three oxidative peaks (A3, A2 and A2') disappeared and the peak current of A1 decreased continuously with the rise of 3,6-D concentration in the electrolyte. Moreover, it is noted that a small double-layer charging current was present in the potential range between -0.15 and -0.35 V with the addition of 3,6-D (Fig. 6B), indicating the adsorption of 3,6-D over the Pd/Ni electrode [Eq. 2, Section 1] [48]. This shows the typical CV curves of the ECH dechlorination processes at Pd-modified electrodes [15,17], which strongly suggests that the dechlorination of 3,6-D follows the stated typical ECH mechanism in Section 1.

The potentials of the Pd/Ni foam cathode were more positive than -1.25 V in most aforementioned electrolysis experiments (Section 3.1. and 3.2.. Fig. 7 shows the typical CP curves of Pd/Ni foam cathodes in a 1.25 M NaOH aqueous solution in the presence of 250 mM 3,6-D. The applied potential during electrolysis mainly ranged from -1.0 V to -1.25 V.). Therefore, the CV curves (Fig. 6) with a limited negative potential of -1.25 V are valid to reflect the dechlorination mechanism of 3,6-D on the Pd/Ni foam cathode.

3.3.2. Surface morphology, composition and phase of Pd/Ni cathode

According to the stated ECH mechanism, the relative rates of hydrogenation (Eq. 3) and H_2 desorption steps (Eqs. 5 and 6) determines the dechlorination efficiency of Pd/Ni foam cathode; thus, the factors that influence these two steps would affect the dechlorination efficiency of 3,6-D [16].



Both the hydrogenation and H_2 desorption steps occurred on the surface of Pd/Ni cathode. Therefore, the surface morphology, composition and phase of Pd/Ni cathode must be very important factors that strongly influence the dechlorination efficiency of Pd/Ni foam cathode. As shown in the SEM pictures of Fig 8, the surface of Ni foam

was covered with an obvious film after the metallic replacement reaction. Because EDS and XPS (Fig 8) gave a similar surface Ni/Pd ratio of approximate 3/7 for the Pd/Ni foam, it is believed that the thickness of the film was up to a few microns, and the film had a uniform Ni/Pd ratio in depth. In addition, given that no diffraction peak corresponding to Pd-Ni alloy was observed in the XRD pattern of the Pd/Ni foam (Fig. 9), the possibility of having a Pd-Ni alloy was omitted. Based on these results, the surface of Pd or the interface of Pd-Ni bimetallic contact was assumed to be the main reaction site for the ECH dechlorination of 3,6-D. Unfortunately, it is not possible to discriminate between these two reaction sites on the basis of the data so far available.

3.3.3. Effect of catholyte pH

Catholyte pH not only influences the adsorption of H (Eq. 1) but may also change the molecular structure and adsorption behavior of 3,6-D [49], making it another important factor that can significantly change the rate of hydrogenation step and dechlorination route. Two Cl atoms in the 3,6-D molecule were eliminated stepwise in 1.25 M NaOH, whereas the atoms were removed together in one step in 0.75 M H₂SO₄ (Section 3.2.1.). In order to rationalize the abovementioned significant difference in the dechlorination route, the molecular structure and two C-Cl bonds length of 3,6-D were calculated by DFT. In the alkaline environment, 3,6-D is in an anionic form. The bond length of C₆-Cl is longer than that of C₃-Cl for 0.027 Å (Table 4). In strong acidic solution, however, 3,6-D is cationic as carboxylate ion and the pyridinic nitrogen are both protonated [49]. In contrast, the bond length difference of C₆-Cl and C₃-Cl are very small (only 0.011 Å). On the basis of these results, we believe that the different molecular structure of 3,6-D in different pH solutions was one of the essential reasons for the different dechlorination route.

The difference in dechlorination route may also resulted from a change in the surface adsorption geometry of 3,6-D on the used Pd/Ni cathode along with the change of pH value. In 1.25 M NaOH, 3,6-D was mainly adsorbed on the cathode surface through Cl at C₆ to minimize the electrostatic repulsion between 3,6-D and the cathode as the COO⁻ of 3,6-D is completely unprotonated [50]. Thus, the Cl at C₆ was

dechlorinated preferentially. In 0.75 M H₂SO₄, however, electrostatic repulsion became weaker because of the protonation of COO⁻ and pyridinic nitrogen [49,50]. Therefore, both the Cl at C₆ and the Cl at C₃ of 3,6-D can be adsorbed on the cathode, thereby eliminating the two Cl atoms in the molecule of 3,6-D in one step. Based on the discussion regarding the CV data, the dechlorination route and the electrode surface characteristic, the ECH dechlorination mechanism of 3,6-D on the Pd/Ni foam cathode is proposed in Fig. 10.

3.4. Rate-limiting step

3.4.1. CV evidence

According to the stated ECH mechanism in Section 1, the hydrogenation step (Eq. 3) in the presence of 3,6-D would consume the adsorbed hydrogen, reduce the concentration of adsorbed hydrogen, and accelerate the electro-adsorption of hydrogen. This explains why the addition of 3,6-D increased the reductive peak (C1) at the expense of the oxidative peaks (A1, A2, A2' and A3) (Fig. 6B). The current of the reductive peak (C1) shows a trend of first increased quickly and then increased slowly when the concentration of 3,6-D increased from 0 mM to 100 mM and then from 100 mM to 250 mM, suggesting that the ECH dechlorination process was kinetically limited by a surface reaction step at the high reactant concentration whereas partially by a diffusion step of 3,6-D from bulk catholyte to the cathode surface at the low reactant concentration.

3.4.2. Effect of 3,6-D initial concentration

Four surface reaction steps (Eqs. 1–4) are included in the ECH dechlorination process of 3,6-D. Among these steps, the adsorption of 3,6-D was influenced directly by the 3,6-D concentration in the bulk catholyte. Therefore, the concentration of 3,6-D is an important factor that can change the rate-limiting step of the dechlorination process.

As shown in Table 3, over 95% CE was achieved at the initial 3,6-D concentration range of 200 mM to 300 mM (Entries 5–7). This result demonstrates

that the H₂ desorption step (Eqs. [5] and [6]) was almost completely restricted during most of the ECH experiments, which implies that the adsorbed hydrogen was immediately consumed by a very fast hydrogenation step and the concentration of adsorbed hydrogen dropped to near zero on the Pd/Ni foam cathode. Simply put, the generation of adsorbed hydrogen was the rate-limiting step of the dechlorination process under this circumstance. The high concentration of 3,6-D in the bulk catholyte inevitably led to high concentration of 3,6-D on the surface of the Pd/Ni foam cathode because the ECH dechlorination process was not kinetically limited by the diffusion step of 3,6-D. The high concentration of 3,6-D on the surface of the Pd/Ni foam cathode was favorable for the adsorption of 3,6-D, thereby accelerating the hydrogenation step.

At the initial 3,6-D concentration range of 25 mM to 50 mM (Table 3), however, the CE obtained was very low (17.6%–35.7%). This result demonstrates that the concentration of adsorbed hydrogen on the Pd/Ni foam cathode was quite high during the ECH experiments. In other words, the ECH dechlorination process was not limited by the generation of adsorbed hydrogen under such a condition. Using the same theory, low concentrations of 3,6-D in the bulk catholyte inevitably resulted in low concentrations of 3,6-D on the surface of the Pd/Ni foam cathode, which is unfavorable for both the adsorption of 3,6-D and the hydrogenation step. Therefore, these two steps or the diffusion step of 3,6-D from bulk catholyte to the cathode surface were most likely the rate-limiting steps of the dechlorination in the presence of low 3,6-D concentrations.

3.4.3. Effect of applied current density

The current density would affect the ECH dechlorination by directly controlling the generation rate of adsorbed hydrogen. Therefore, current density is another important factor that might change the rate-limiting step of the ECH dechlorination process.

As shown in Fig. 5(A), over 94% CE was achieved during the whole electrolysis experiment of 250 mM 3,6-D at the current density of 83 A m⁻². This result suggests

that the hydrogenation step was faster than the generation of adsorbed hydrogen under such a condition, and the ECH dechlorination process was kinetically controlled by the generation of adsorbed hydrogen.

At the high current density of 250 A m^{-2} , however, a parabolic drop was observed in the CE when electrolysis time was extended. Over 95% CE was achieved during the first two hours of the electrolysis experiment (Fig. 5A). Therefore, the generation of adsorbed hydrogen kinetically controlled the ECH dechlorination at this period of time. A very low CE (lower than 30%) was obtained during the last hour of the electrolysis experiment (Fig. 5C), which indicates that the generation rate of the adsorbed hydrogen was faster than that of the hydrogenation step. Therefore, the hydrogenation step and/or adsorption of 3,6-D was most likely the rate-limiting step of the dechlorination process under such a condition. The shift of the rate-limiting step during the electrolysis experiment resulted from the decrease of 3,6-D concentration in the catholyte when the electrolysis time was extended (Fig. 5D), thereby decreasing the rate of adsorption of 3,6-D and the hydrogenation step.

3.5. ECH dechlorination of the CIPA mixtures

Using the optimized experimental conditions (7 cm \times 13 cm Pd/Ni foam with a Pd loading of 2.25 mg cm^{-2} used as the cathode, 700 mL 1.25 M NaOH aqueous solution as the catholyte, 208 A m^{-2} as the applied current density), the practicability of the ECH dechlorination system to convert the CIPA mixtures to PA was assessed using a plate-and-frame cell at a flow rate of 1.2 L/min.

After ECH dechlorination for 12 h, four CIPAs in the catholyte (total concentration of CIPAs was approximately 250 mM) were converted to PA with 99% PA yield, 76.3% CE, and $2.47 \text{ kW}\cdot\text{h}\cdot\text{kg}^{-1}$ PA SEEC. These technical indexes indicate that the ECH dechlorination system is likely to be high economic value, considering that the price of commercial electric energy and PA is approximately 0.12 USD per $(\text{kW}\cdot\text{h})^{-1}$ and 30 USD per kg in China, respectively. Besides electric energy, the cost of electrode materials (especially the cost of Pd), chemical reagents used for pH adjustment should be carefully assessed, if we plan to put the ECH dechlorination

system into industrial applications.

High current density and high CE are very important for practical electrolysis techniques, which not only reduce the dosage of catalyst but also increase the space-time yield of an electrolysis reactor. As shown in the ECH dechlorination of the ClPA mixtures, high CE (76.3%) was achieved at an acceptable current density (208 A m⁻²) when high concentration (250 mM) of reactants was used. These results suggest that the ECH dechlorination system developed in this work can be potentially used in industrial applications for the dechlorination of ClPA mixtures to PA and even for the disposal of other high concentration COCs that are soluble in basic aqueous solutions, such as chlorinated phenols, chlorinated phenoxyacetic acids, and chloracetic acids.

4. Conclusion

A highly efficient ECH dechlorination system (1.25 M NaOH aqueous solution as the catholyte, Pd/Ni foam as the cathode) was developed for the dechlorination of a ClPA mixtures into PA. This goal was achieved by using 3,6-D as the target compound and optimizing the Pd loading, its cathode support (Ni foam, Ag mesh, and Cu foam), and operating parameters, such as catholyte pH, initial reactant concentration, and applied current density. We also investigated the dechlorination mechanism of 3,6-D with regard to the surface condition of cathode and catholyte pH, the rate-limiting step of the dechlorination process, and the practicability of the optimized ECH dechlorination system to convert the ClPA mixtures into PA. The main findings are as follows:

(1) The activity of six metal cathodes during the dechlorination of 3,6-D in 0.5 M NaOH aqueous solution decreased in the following order: Pd/Ni foam > Pd/Ag mesh \approx Pd/Cu foam \gg Ni foam \approx Ag mesh \approx Cu foam, and the Pd/Ni foam cathodes with a Pd loading of 2.25–3.6 mg cm⁻² exhibited the optimum dechlorination performance. The dechlorination of 3,6-D on the Pd/Ni foam cathodes was confirmed as a typical ECH process, and the surface of Pd or the interface of Pd-Ni bimetallic contact was probably the main ECH site.

(2) The dechlorination efficiency increased with the rise of the initial concentration of 3,6-D (from 25–200 mM). The initial 3,6-D concentration region of 200–300 mM exhibited the highest dechlorination efficiency, which indicates that higher initial concentrations (< 300 mM) favor the ECH dechlorination of 3,6-D on the Pd/Ni foam cathode. The current density also considerably affected the dechlorination reactions, as a moderate current density (208 A m^{-2}) exhibited the highest dechlorination efficiency.

(3) The intermediate product selectivity and efficiency of the ECH dechlorination system strongly depended on the catholyte pH values. The highest dechlorination efficiency was achieved in 1.25 M NaOH or 0.75 M H_2SO_4 . Two Cl atoms in the 3,6-D molecule were eliminated stepwise in 1.25 M NaOH, whereas the atoms were removed together in one step in 0.75 M H_2SO_4 . This result may be associated with the change in the molecular structure or the surface adsorption geometries of 3,6-D on the Pd/Ni foam cathode.

(4) The rate-limiting step of the dechlorination process changed along with the variation of reactant concentration in the catholyte and applied current density. The dechlorination process was kinetically limited by the generation of adsorbed hydrogen at low applied current density, whereas it may have been kinetically limited by the hydrogenation step and/or adsorption of reactants or the diffusion step of 3,6-D from bulk catholyte to the cathode surface at low concentration of reactants in return.

(5) The practicability research demonstrated that the 47 g L^{-1} CIPA mixtures (total concentration of CIPAs: approximately 250 mM) can be converted into PA with 99% yield, 76.3% CE, and $2.47 \text{ kW}\cdot\text{h}\cdot\text{kg}^{-1}$ PA SEEC in the optimized ECH dechlorination system. This finding indicated that the ECH dechlorination system developed in this work presents a considerable potential in industrial applications.

For future studies, this ECH dechlorination system can be adjusted for the disposal of other high-concentration COCs, which are soluble in basic aqueous solutions, such as chlorinated phenols, chlorinated phenoxyacetic acids, and chloroacetic acids.

Acknowledgments

This work was supported by the National Natural Science Foundation of China (21106133, 21207028, and 21576238), the Natural Science Foundation of Zhejiang Province, China (LY16B060012), and the National Basic Research Program of China (973 Program) (2012CB722604).

References

- [1] Public announcement of project acceptance accomplishing environmental protection installation, Environmental Protection Agency, Zhejiang Province, 2013, http://www.zjepb.gov.cn/root14/xxgk/xzxk/xzxkspgs/jsxmhbhssjgys/201311/t20131120_294868.html.
- [2] Public announcement of project acceptance accomplishing environmental protection installation, Environmental Protection Agency, Mianyang City, 2014, <http://www.my.gov.cn/MYGOV/150650805483995136/20140815/1117055.html>.
- [3] Public announcement of project acceptance accomplishing environmental protection installation, Environmental Protection Agency, Zhangjiakou City, 2014, <http://www.zjkepb.gov.cn/show.aspx?id=12179&cid=35>.
- [4] C.A. Ma, Y.H. Xu, Y.Q. Chu, X.B. Mao, F.M. Zhao, Y.H. Zhu, Electrochemical synthesis of 3,6-dichloropicolinic acid and its industrialization, *CIES J.* 61 (2010) 699–703.
- [5] D.V. Sojic, V.B. Anderluh, D.Z. Orcic, B.F. Abramovic, Photodegradation of clopyralid in TiO₂ suspensions: Identification of intermediates and reaction pathways, *J. Hazard. Mater.* 168 (2009) 94–101.
- [6] K. Westphal, R. Saliger, D. Jager, L. Teevs, L. Teevs, U. Pruße, Degradation of clopyralid by the Fenton reaction, *Ind. Eng. Chem. Res.* 52 (2013) 13924–13929.
- [7] G. Xu, T. Bu, M. Wu, J. Zheng, N. Liu, L. Wang, Electron beam induced degradation of clopyralid in aqueous solutions, *J. Radioanal. Nucl. Chem.* 288 (2011)

759–764.

- [8] C. Tizaoui, K. Mezughi, R. Bickley, Heterogeneous photocatalytic removal of the herbicide clopyralid and its comparison with UV/H₂O₂ and ozone oxidation techniques, *Desalination* 273 (2011) 197–204.
- [9] S.Q. Wang, J.Z. He, Dechlorination of commercial PCBs and other multiple halogenated compounds by a sediment-free culture containing dehalococcoides and dehalobacter, *Environ. Sci. Technol.* 47 (2013) 10526–10534.
- [10] J. Farrell, M. Kason, N. Melitas, T. Li, Investigation of the long-term performance of zero-valent iron for reductive dechlorination of trichloroethylene, *Environ. Sci. Technol.* 34 (2000) 514–521.
- [11] Y. Kim, E.R. Carraway, Dechlorination of pentachlorophenol by zero valent iron and modified zero valent irons, *Environ. Sci. Technol.* 34 (2000) 2014–2017.
- [12] L. Teevs, K.-D. Vorlp, U. Pruße, Model study on the aqueous-phase hydrodechlorination of clopyralid on noble metal catalysts, *Catal. Commun.* 14 (2011) 96–100.
- [13] C. Sun, Z.M. Lou, Y. Liu, R.Q. Fu, X.X. Zhou, Z. Zhang, S.A. Baig, X.H. Xu, Influence of environmental factors on the electrocatalytic dechlorination of 2,4-dichlorophenoxyacetic acid on nTiN doped Pd/Ni foam electrode, *Chem. Eng. J.* 281 (2015) 183–191.
- [14] C. Sun, S.A. Baig, Z.M. Lou, J. Zhu, Z.X. Wang, X. Li, J.H. Wu, Y.F. Zhang, X.H. Xu, Electrocatalytic dechlorination of 2,4-dichlorophenoxyacetic acid using nanosized titanium nitride doped palladium/nickel foam electrodes in aqueous solutions, *Appl. Catal. B: Environ.* 158–159 (2014) 38–47.
- [15] I.G. Casella, M. Contursi, Electrocatalytic reduction of chlorophenoxy acids at palladium-modified glassy carbon electrodes, *Electrochim. Acta* 52 (2007) 7028–7034.
- [16] Y.H. Xu, Q.Q. Cai, H.X. Ma, Y. He, H. Zhang, C.A. Ma, Optimisation of electrocatalytic dechlorination of 2,4-dichlorophenoxyacetic acid on a roughened silver–palladium cathode, *Electrochim. Acta* 96 (2013) 90–96.
- [17] C.A. Ma, H. Ma, Y.H. Xu, Y.Q. Chu, F.M. Zhao, The roughened

silver-palladium cathode for electrocatalytic reductive dechlorination of 2,4-Dichlorophenoxyacetic acid, *Electrochem. Commun.* 11 (2009) 2133–2136.

[18] W.J. Li, H.Y. Ma, L.H. Huang, Y. Ding, Well-defined nanoporous palladium for electrochemical reductive dechlorination, *Phys. Chem. Chem. Phys.* 13 (2011) 5565–5568.

[19] W.J. Xie, S.H. Yuan, X.H. Mao, W. Hu, P. Liao, M. Tong, A.N. Alshwabkeh, Electrocatalytic activity of Pd-loaded Ti/TiO₂ nanotubes cathode for TCE reduction in groundwater, *Water Res.* 47 (2013) 3573–3582.

[20] I.S. Park, K.S. Lee, S.J. Yoo, Y.H. Cho, Y.E. Sung, Electrocatalytic properties of Pd clusters on Au nanoparticles in formic acid electro-oxidation, *Electrochim. Acta* 55 (2010) 4339–4345.

[21] I.F. Cheng, Q. Fernando, N. Korte, Electrochemical dechlorination of 4-chlorophenol to phenol, *Environ. Sci. Technol.* 31 (1997) 1074–1078.

[22] Z. Sun,; H. Ge, X. Hu, Y. Peng, Electrocatalytic Dechlorination of Chloroform in Aqueous Solution on Palladium/Titanium Electrode, *Chem. Eng. Technol.* 32(2009) 134–139.

[23] H. Cheng, K. Scott, P.A. Christensen, Electrochemical Hydrodehalogenation of Chlorinated Phenols in Aqueous Solutions II. Effect of Operating Parameters, *J. Electrochem. Soc.* 150 (2003) D25-D29.

[24] B. Yang, G. Yu, D.M. Shuai, Electrocatalytic hydrodechlorination of 4-chlorobiphenyl in aqueous solution using palladized nickel foam cathode, *Chemosphere* 67 (2007) 1361-1367.

[25] B. Yang, G. Yu, J. Huang, Electrocatalytic Hydrodechlorination of 2,4,5-Trichlorobiphenyl on a Palladium-Modified Nickel Foam Cathode, *Environ. Sci. Technol.* 41 (2007) 7503-7508.

[26] K.R. Zhu, C. Sun, H. Chen, S.A. Baig, T.T. Sheng, X.H. Xu, Enhanced catalytic hydrodechlorination of 2,4-dichlorophenoxyacetic acid by nanoscale zero valent iron with electrochemical technique using a palladium/nickel foam electrode, *Chem. Eng. J.* 223 (2013) 192–199.

[27] Z.Q. He, J.J. Sun, J. Wei, Q. Wang, C.X. Huang, J.M. Chen, S. Song, Effect of

silver or copper middle layer on the performance of palladium modified nickel foam electrodes in the 2-chlorobiphenyl dechlorination, *J. Hazard. Mater.* 250–251 (2013) 181–189.

[28] P. Dabo, A. Cyr, F. Laplante, F. Jean, H. J. Menard, Lessard, Electrocatalytic dehydrochlorination of pentachlorophenol to phenol or cyclohexanol, *Environ. Sci. Technol.* 34 (2000) 1265–1268.

[29] G. Chen, Z.Y. Wang, D.G. Xia, Electrochemically codeposited palladium/molybdenum oxide electrode for electrocatalytic reductive dechlorination of 4-chlorophenol, *Electrochem. Commun.* 6 (2004) 268–272.

[30] M. Kuroboshi, H. Idei, N. Kara, Y. Kokui, H. Yanaka, Electroreduction of aryl halides loaded on palladium-immobilized activated carbon, *Electrochemistry* 81 (2013) 359–361.

[31] A.I. Tsyganok, K. Otsuka, Selective dechlorination of chlorinated phenoxy herbicides in aqueous medium by electrocatalytic reduction over palladium-loaded carbon felt, *Appl. Catal. B: Environ.* 22 (1999) 15–26.

[32] Y.X. Fang, S.R. Al-Abed, Electrocatalytic dechlorination of a PCB congener at a palladized granular-graphite-packed electrode: Reaction equilibrium and mechanism, *Appl. Catal. B: Environ.* 80 (2008) 327–334.

[33] C.Y. Cui, X. Quan, H.T. Yu, Y.H. Han, Electrocatalytic hydrodehalogenation of pentachlorophenol at palladized multiwalled carbon nanotubes electrode, *Appl. Catal. B: Environ.* 80 (2008) 122–128.

[34] Q. Shi, H. Wang, S. Liu, Z. Bian, Electrocatalytic degradation of 2,4-dichlorophenol using a Pd/grapheme gas-diffusion electrode, *RSC Adv.*, 4 (2014) 56263–56272.

[35] Q. Shi, H. Wang, S. Liu, L. Pang, Z. Bian, Electrocatalytic reduction-oxidation of chlorinated phenols using a nanostructured Pd-Fe modified graphene catalyst, *Electrochim. Acta* 178 (2015) 92–100.

[36] G. Chen, Z.Y. Wang, T. Yang, D.D. Huang, D.G. Xia, Electrocatalytic hydrogenation of 4-chlorophenol on the glassy carbon electrode modified by composite polypyrrole/palladium film, *J. Phys. Chem. B* 110 (2006) 4863–4868.

- [37] Z.R. Sun, H. Ge, X. Hu, Y.Z. Peng, Preparation of foam-nickel composite electrode and its application to 2,4-dichlorophenol dechlorination in aqueous solution, *Sep. Purif. Technol.* 72 (2010) 133-139.
- [38] Z.R. Sun, X.F. Wei, H.T. Shen, X. Hu, Preparation and evaluation of Pd/polymeric pyrrole-sodium lauryl sulfonate/foam-Ni electrode for 2,4-dichlorophenol dechlorination in aqueous solution, *Electrochim. Acta* 129 (2014) 433–440.
- [39] Z.R. Sun, X.F. Wei, Y.B. Han, S.Tong, X. Hu, Complete dechlorination of 2,4-dichlorophenol in aqueous solution on palladium/polymeric pyrrole-cetyltrimethyl ammonium bromide/foam-nickel composite electrode, *J. Hazard. Mater.* 244–245 (2013) 187–194.
- [40] Z.R. Sun, H.T. Shen, X.F. Wei, X. Hu, Electrocatalytic hydrogenolysis of chlorophenols in aqueous solution on Pd₅₈Ni₄₂ cathode modified with PPy and SDBS, *Chem. Eng. J.* 241 (2014) 433–442.
- [41] T. Yanai, D.P. Tew, N.C. Handy, A new hybrid exchange-correlation functional using the Coulomb-attenuating method (CAM-B3LYP), *Chem. Phys. Lett.* 393 (2004) 51-57.
- [42] R. Krishnan, J. S. Binkley, R. Seeger, J.A. Pople, Self-consistent molecular orbital methods. XX. A basis set for correlated wave functions, *J. Chem. Phys.* 72 (1980) 650-654.
- [43] M.J. Frisch, G.W. Trucks, H. B. Schlegel, *et al.* *Gaussian 03*, Revision C.01; Gaussian Inc.: Pittsburgh, PA, 2003.
- [44] S. Wang, B. Yang, T.T. Zhang, G. Yu, S.B. Deng, J. Huang, Catalytic Hydrodechlorination of 4-Chlorophenol in an Aqueous Solution with Pd/Ni Catalyst and Formic Acid, *Ind. Eng. Chem. Res.* 49 (2010), 4561–4565.
- [45] E. Diaz, J.A. Casas, A.F. Mohedano, L. Calvo, M. A. Gilarranz, J.J. Rodriguez, Kinetics of the Hydrodechlorination of 4-Chlorophenol in Water Using Pd, Pt, and Rh/Al₂O₃ Catalysts, *Ind. Eng. Chem. Res.* 47 (2008), 3840–3846.
- [46] J.A. Baeza, L. Calvo, M.A. Gilarranz, A.F. Mohedano, J.A. Casas, J.J. Rodriguez, Catalytic behavior of size-controlled palladium nanoparticles in the

- hydrodechlorination of 4-chlorophenol in aqueous phase, *J. Catal.* 293 (2012) 85–93.
- [47] G. Denuault, C. Milhano, D. Pletcher, Mesoporous palladium—the surface electrochemistry of palladium in aqueous sodium hydroxide and the cathodic reduction of nitrite, *Phys. Chem. Chem. Phys.* 7 (2005) 3545-3551.
- [48] S.L. Yau, Y.G. Kim, K.J. Itaya, In situ scanning tunneling microscopy of benzene adsorbed on Rh (111) and Pt (111) in HF solution. *J. Am. Chem. Soc.* 118, (1996) 7795–7803.
- [49] Y.H. Xu, X.F. Ding, H.X. Ma, Y.Q. Chu, C.A. Ma, Selective hydrodechlorination of 3,5,6-trichloropicolinic acid at an activated silver cathode: Synthesis of 3,5-dichloropicolinic acid, *Electrochim. Acta* 151 (2015) 284–288.
- [50] M.C. Corredor, J.M.R. Mellado, M.R. Montoya, EC(EE) process in the reduction of the herbicide clopyralid on mercury electrodes, *Electrochim. Acta* 51 (2006) 4302–4308.

Figure captions

Fig. 1. Schematic construction of the electrolysis device by using a plate-and-frame cell.

Fig. 2. Effect of Pd loading on the electrolysis of 3,6-D. Cathode: Pd/Ni foams (Projected area: 2 cm × 6 cm); Catholyte: 50 mL 0.5 M NaOH + 0.25 M 3,6-D; Anode: graphite sheet (2 cm × 6 cm × 0.5 cm); Anolyte: 50 mL 1.25 M NaOH; Applied current: 0.25 A (208 A m⁻²); Electrolysis time: 6 h; Temperature: 25 °C. CE was calculated with $\Delta t = 6$ h.

Fig. 3. Stability of Pd/Ni foam cathode over six cycles of electrolysis. The projected area of the Pd/Ni foam cathode: 2 cm × 6 cm; Pd loading: 2.25 mg cm⁻²; Catholyte: 50 mL 0.5 M NaOH + 0.25 M 3,6-D; Anode: graphite sheet (2 cm × 6 cm × 0.5 cm); Anolyte: 50 mL 1.25 M NaOH; Applied current: 0.25 A (208 A m⁻²); Electrolysis time of each run: 6 h; Temperature: 25 °C. CE was calculated with $\Delta t = 6$ h.

Fig. 4. Effect of pH on product selectivity and CE during the electrolysis of 3,6-D. Cathode: Pd/Ni foams (Projected area: 2 cm × 6 cm, Pd loading: 2.25 mg cm⁻²); Catholyte: (A and A') 50 mL 1.25 M NaOH + 96 mM 3,6-D, (B and B') 50 mL 0.75 M H₂SO₄ + 96 mM 3,6-D+ 20% v/v Ethanol; Anode: graphite sheet (2 cm × 6 cm × 0.5 cm); Anolyte: 50 mL 1.25 M NaOH for A, and 50 mL 0.75 M H₂SO₄ for B; Applied current: 0.1 A; Temperature: 25 °C; CE was calculated with $\Delta t = 1$ h.

Fig. 5. Effect of current density on CE, yield of PA, and conversion of 3,6-D during the electrolysis of 3,6-D. (A) Partially enlarged drawing of (C). Cathode: Pd/Ni foams (Projected area: $2\text{ cm} \times 6\text{ cm}$, Pd loading: 2.25 mg cm^{-2}); Catholyte: $50\text{ mL } 1.25\text{ M NaOH} + 250\text{ mM } 3,6\text{-D}$; Anode: graphite sheet ($2\text{ cm} \times 6\text{ cm} \times 0.5\text{ cm}$); Anolyte: $50\text{ mL } 1.25\text{ M NaOH}$; Temperature: $25\text{ }^{\circ}\text{C}$; CE was calculated with $\Delta t = 1\text{ h}$.

Fig. 6. CV curves of Pd/Ni disk (3 mm diameter) in a 1.25 M NaOH aqueous solution (A) with different negative limit; (B) with various concentrations of 3,6-D, at a scan rate of $100\text{ mV}\cdot\text{s}^{-1}$.

Fig. 7. Typical chronopotentiometry (CP) curves during the electrolysis at 25°C . Cathode: Pd/Ni foams (Projected area: $2\text{ cm} \times 6\text{ cm}$, Pd loading: 2.25 mg cm^{-2}); Catholyte: $50\text{ mL } 1.25\text{ M NaOH} + 0.25\text{ M } 3,6\text{-D}$; Anode: graphite sheet ($2\text{ cm} \times 6\text{ cm} \times 0.5\text{ cm}$); Anolyte: $50\text{ mL } 1.25\text{ M NaOH}$; Applied current: 0.25 A (208 A m^{-2}).

Fig. 8. SEM images and EDS of a Ni foam and a Pd/Ni foam, and XPS images of Pd/Ni foam (Pd loading: 2.25 mg cm^{-2}).

Fig. 9. XRD patterns of (A) a Ni foam and (B) a Pd/Ni foam (Pd loading: 2.25 mg cm^{-2}).

Fig. 10. Proposed mechanisms for the ECH dechlorination of 3,6-D.

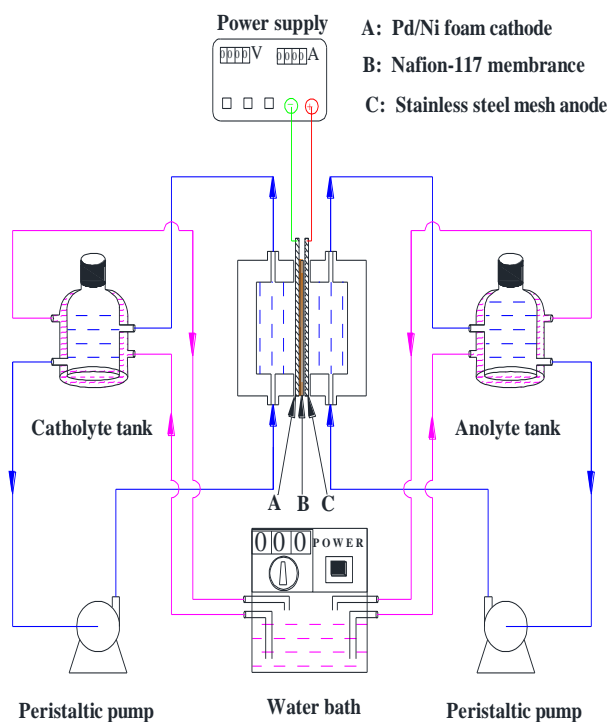
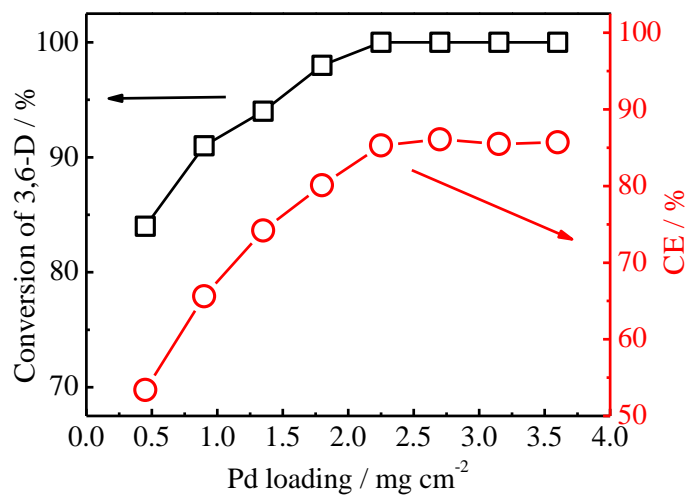
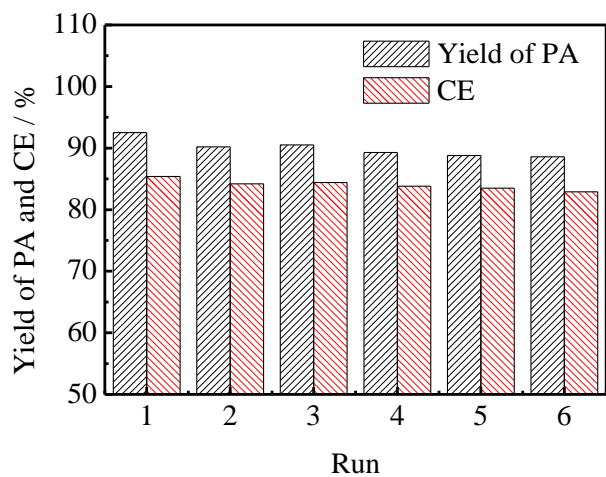


Fig. 1

**Fig. 2****Fig. 3**

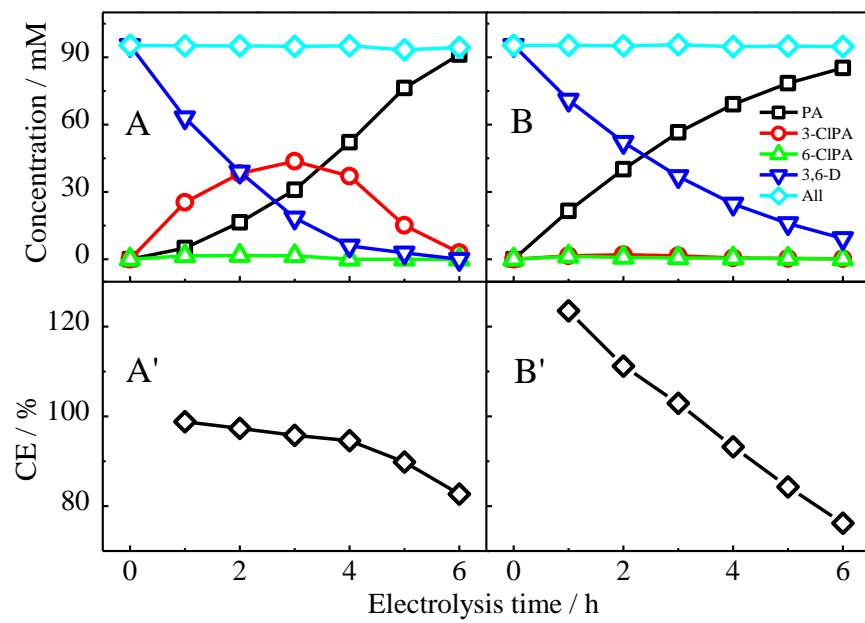


Fig. 4

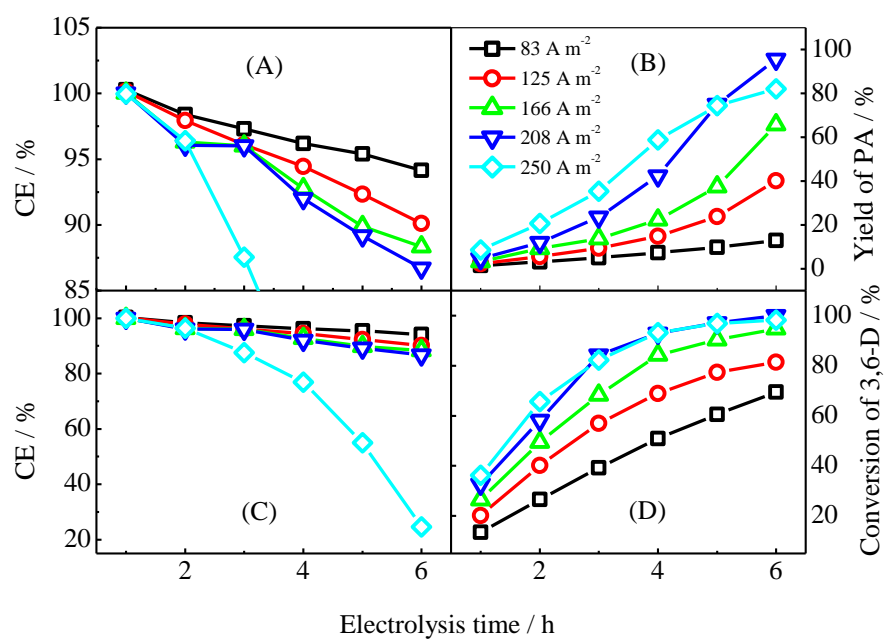


Fig. 5

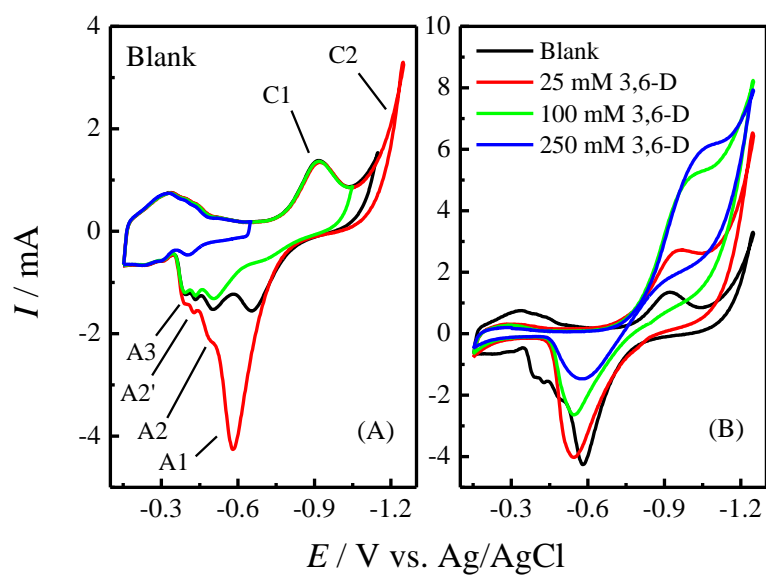


Fig. 6

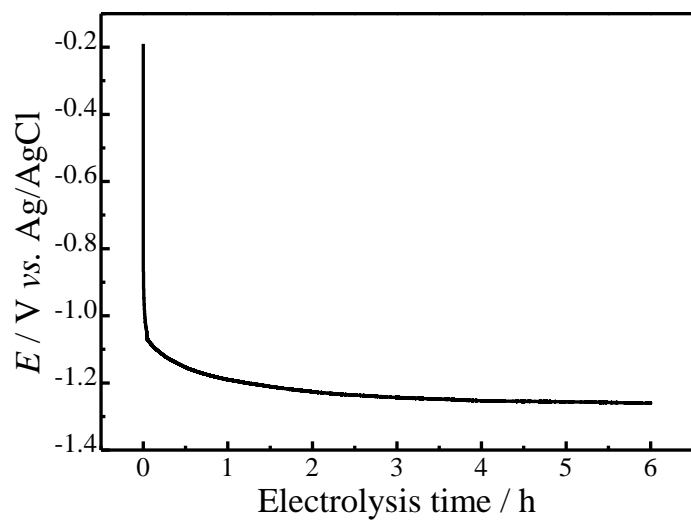


Fig. 7

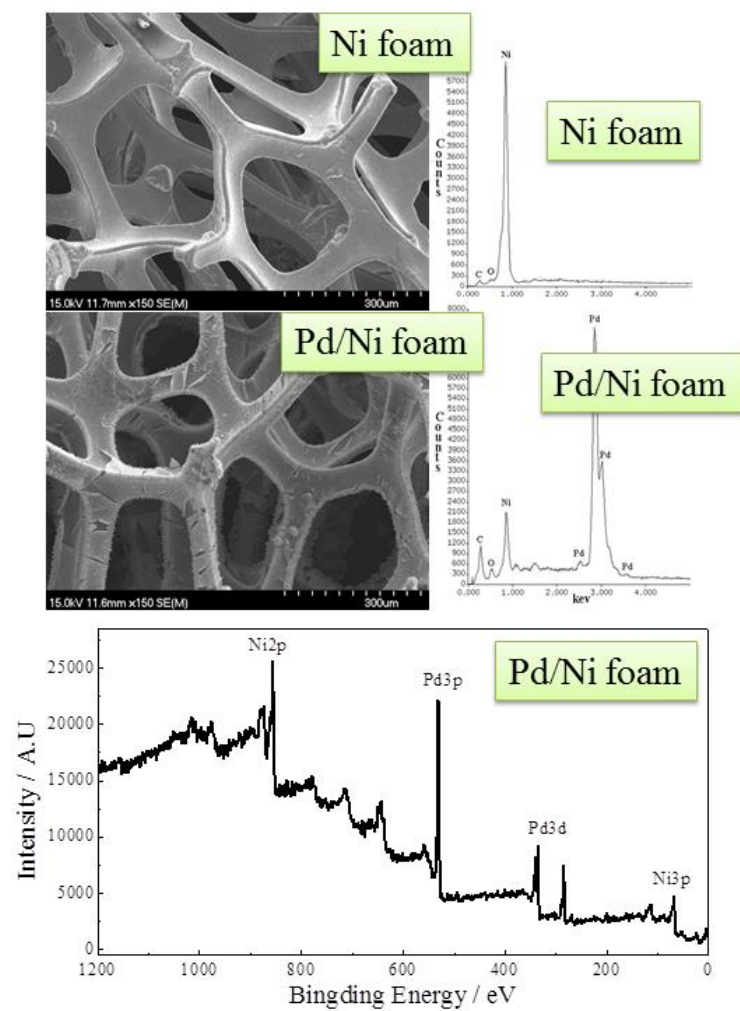


Fig. 8

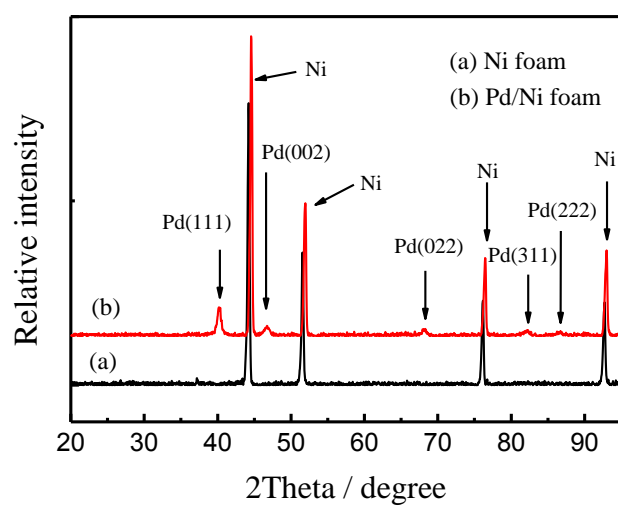


Fig. 9

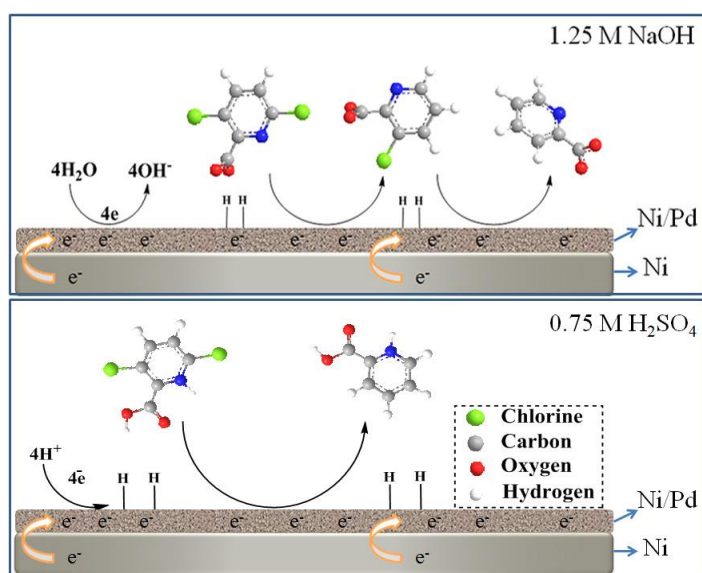


Fig. 10

Table 1 Effect of cathode supports on the electrolysis of 3,6-D.^a

Entry	Cathode ^b	Final product distribution (%)				CE ^c (%)
		3,6-D	PA	3-CIPA	6-CIPA	
1	Pd/Ni foam	0	92.3	6.4	0	85.3
2	Pd/Ag mesh	11.1	31.8	55.9	1.1	53.9
3	Pd/Cu foam	18.5	50.8	32.7	1.3	60.6
4	Ni foam	92.0	0	1.7	2.9	2.1
5	Ag mesh	95.8	0	0.9	3.6	2.0
6	Cu foam	94.8	0	1.2	2.9	1.8

^a Catholyte: 50 mL 0.5 M NaOH + 0.25 M 3,6-D; Anode: graphite sheet (2 cm × 6 cm × 0.5 cm); Anolyte: 50 mL 1.25 M NaOH; Applied current: 0.25 A (208 A m⁻²); Electrolysis time: 6.0 h; Temperature: 25 °C.

^b The projected area of six electrodes is 2 cm × 6 cm; and the Pd loading of Pd/Ni foam, Pd/Ag mesh, and Pd/Cu foam electrodes are 2.25 mg cm⁻².

^c CE was calculated with $\Delta t = 6.0$ h.

Table 2 Effect of electrolyte pH on the electrolysis of 3,6-D.^a

Entry	Catholyte ^b	pH	Final product distribution (%)				CE ^c (%)
			3,6-D	PA	3-CIPA	6-CIPA	
1	1.25M NaOH+ 0.25 M 3,6-D	/	0	95.5	3.7	0	86.9
2	0.5 M NaOH + 0.25 M 3,6-D	13.1–14	0	92.3	6.4	0	85.3
3	0.25 M NaOH + 0.25 M 3,6-D	11.5–13.5	0	88.3	10.9	0	83.7
4	0.5 M KH ₂ PO ₄ + 0.3 M NaOH + 0.25 M 3,6-D	7.2–9.4	14.9	54.1	29.2	0.3	61.5
5	0.5 M KH ₂ PO ₄ + 0.2 M NaOH+ 0.25 M 3,6-D	4.4–6.6	46.6	35.5	17.6	0.2	39.7
6	0.5 M KH ₂ PO ₄ + 0.2 M NaOH+ 0.25 M 3,6-D	4.4–1.3	9.3	88.1	2.3	0	79.7
7 ^d	0.75 M H ₂ SO ₄ + 20 % v/v Ethanol + 0.25 M 3,6-D	/	3.9	93.8	2.1	0	84.7

^a Cathode: Pd/Ni foam (Projected area: 2 cm × 6 cm, Pd loading: 2.25 mg cm⁻²); Anode: graphite sheet (2 cm × 6 cm × 0.5 cm); Anolyte: 50 mL 1.25M NaOH for entries 1–5, 50 mL 0.75 M H₂SO₄ for entries 6 and 7; Applied current: 0.25 A (208 A m⁻²); Electrolysis time: 6 h; Temperature: 25 °C.

^b The volume of catholyte was 50 mL.

^c CE was calculated with $\Delta t = 6$ h.

^d 3,6-D was added into the catholyte in a divided fashion during the first hour of electrolysis because of its poor solubility.

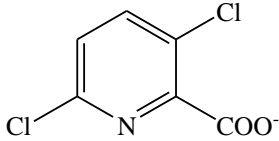
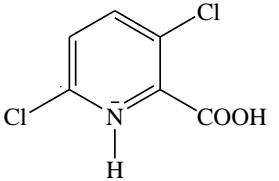
Table 3 Effect of initial concentration on the electrolysis of 3,6-D.^a

Entry	Initial concentration (mM)	Final product distribution (%)				CE ^b (%)
		3,6-D	PA	3-CIPA	6-CIPA	
1	25	0	98.1	1.8	0	17.6
2	50	0	99.8	0.2	0	35.7
3	100	0	91	8.3	0	68
4	150	0.1	70.6	28.9	0	91.2
5	200	7.3	40.9	50.1	1.5	95.3
6	250	15.7	23.4	59.2	1.5	96
7	300	25.6	16.4	55.9	1.1	96.3

^a Cathode: Pd/Ni foam (Projected area: 2 cm × 6 cm, Pd loading: 2.25 mg cm⁻²); Catholyte: 50 mL 1.25 M NaOH + X mM 3,6-D; Anode: graphite sheet (2 cm × 6 cm × 0.5 cm); Anolyte: 50 mL 1.25M NaOH; Applied current: 0.25 A (208 A m⁻²); Electrolysis time: 3.0 h; Temperature: 25 °C.

^b CE was calculated with $\Delta t = 3.0$ h.

Table 4 Molecular structure and C-Cl bond length (Å) of 3,6-D deduced by DFT.

Condition		In 1.25 M NaOH solution	In 0.75 M H ₂ SO ₄ solution
Molecular structure of 3,6-D			
C-Cl bond length (Å)	C ₃ -Cl	1.761	1.716
	C ₆ -Cl	1.788	1.705
	Δ (C-Cl)	0.027	0.011